A R C H I V E S O F M E T A L L U R G Y A N D M A T E R I A L S
Volume 53 2008 Issue 4

D. V. MALAKHOV*

ON A SHAPE-PRESERVING THERMODYNAMIC OPTIMIZATION

O ZACHOWANIU KSZTAŁTU GRANIC MIĘDZYFAZOWYCH W TRAKCIE OPTYMALIZACJI TERMODYNAMICZNEJ

It is demonstrated that topological constraints can be used to control the sign of the curvature of phase boundaries and thus to preserve their shapes in the course of the thermodynamic optimization. In such a way, the unwanted or suspicious inflection points on the phase boundaries may be avoided.

Keywords: CALPHAD method, phase boundary, shape, curvature, inflection point, topological constraint

Wykazano, że zastosowanie pewnych ograniczeń matematycznych można zastosować do kontroli krzywizny granic międzyfazowych w procesie optymalizacji. W ten sposób można uniknąć pojawiania się niepożądanych punktów przegięcia na granicach międzyfazowych.

1. Introduction

In order to apply computational thermodynamics to real-life problems and trust its conclusions and predictions, reliable descriptions of the Gibbs energies of phases in a system of interest must be built. In practice, these Gibbs energies are constructed *via* a two-step procedure known as the CALPHAD (CALculation of PHase Diagrams) method [1, 2]. Firstly, analytical expressions (models) containing unknown adjustable coefficients (models' parameters) are assigned to phases whose Gibbs energies are to be built. Secondly, experimental data on the thermodynamic properties of phases and heterogeneous mixtures, and conditions of phase equilibria are simultaneously treated within the framework of a non-linear least-squares technique, which results in statistically optimal numerical values of a the coefficients [3]. A crucial question is whether the Gibbs energies yielded by the CALPHAD method can be employed in $x - T - P$ regions in which experiments were not carried out, *i.e.*, in other words, whether they can be extrapolated. Although there is no a rigorous answer to this question, it is likely that if the choice of the models reflected the structural and physical properties of corresponding phases, then a range of their applicability would be wide. If, on the other hand, the choice was prompted by a "mathematical convenience", *i.e.*, if an aphysical formalism was used, then extrapolating may lead to artifacts also known as post-optimization phantoms or unintended equilibria [4, 5]. Among such artifacts, inverted miscibility gaps in the liquid phase at elevated temperatures are seen most frequently; the reasons behind their appearance are well understood [6]. Recently, it was demonstrated that using the topological constraints, the inverted miscibility gaps can be eliminated in the course of the thermodynamic assessment [7, 8]. In this work, the same idea is employed to struggle against a different type of artifacts – suspicious inflection points on phase boundaries.

2. Curvatures of phase boundaries

Before launching a battle against inflection points, it is necessary to accentuate that in many cases, their presence at concentration and temperature dependencies of thermodynamic properties as well as phase boundaries is absolutely normal and anticipated. For instance, a concentration dependence of the Raoultian activity of a component in a binary non-ideal solution inevitably has at least one inflection point. This conclusion instantly follows from an attempt to draw a_i (x_i) connecting the Henrian region where $a_i = \gamma_i^{\infty} x_i$ with the Raoultian

* DEPARTMENT OF MATERIALS SCIENCE AND ENGINEERING, MCMASTER UNIVERSITY HAMILTON, ONTARIO, CANADA

region in which $da_i / dx_i = 1$. The existence of the inflection point does not mean that its position can easily be found. Let us consider a regular solution whose excess Gibbs energy is described by $G^{ex} = \omega x(1 - x)$. In order to find abscissa(s) of inflection point(s) at the concentration dependencies of the activities, one has to solve the equations $d^2a_1 / dx^2 = 0$ and $d^2a_2 / dx^2 = 0$. Recalling that for the regular solution $a_1 = (1 - x)\exp(\alpha x^2)$ and $a_2 = x\exp(\alpha(1 - x)^2)$, where $\alpha \equiv \omega/(RT)$, one can simplify these equations to $2\alpha x^2 (1 - x) - 3x + 1 = 0$ and $2\alpha x(1 - x)^2 + 3x - 2 = 0$. Let us notice that even in a very simple case of the regular solution, the cubic equations have been arrived at. If G^{ex} is described by more sophisticated expressions, then the corresponding equations would be either difficult or impossible to solve algebraically. It can be concluded that determining a number of inflection points and their positions at concentration and temperature dependencies of integral and partial thermodynamic properties is a complicated problem whose solution should almost always be sought for numerically. As shown below, in the case of phase boundaries, a corresponding problem becomes even more intricate.

Since an inflection point is the point at which the curvature of a phase boundary changes its sign, it is necessary to calculate the curvature. It is shown in [9] that even in the simplest case when a binary solution is in equilibrium with a binary stoichiometric compound, the expression for the curvature turns is so cumbersome that it can be dealt with only numerically. It is worth noticing that the calculation of the curvature necessitates computing the molar Gibbs energy of the solution and its eight partial derivatives. Five of these derivatives, namely $\partial G/\partial x$, $\partial G/\partial T$, $\partial^2 G/\partial x \partial T$, $\partial^2 G/\partial T^2$ and $\partial^3 G/\partial x \partial T^2$, can be associated with certain thermodynamic properties (for example $\partial^3 G/\partial x \partial T^2$ can be related to partial molar heat capacities). Three remaining derivatives, namely $\partial^2 G/\partial x^2$, $\partial^3 G/\partial x^3$ and $\partial^3 G/\partial x^2 \partial T$, cannot be linked to measurable properties. Consequently, the curvature of the phase boundary cannot be directly derived from experimental observations only; a thermodynamic model of the phase is required as well. It can be concluded that while the curvature of a phase boundary is calculable if the Gibbs energies of two phases co-existing along it are known (the case when these phases are both binary solutions is considered in the Appendix), there are no simple analytical answers to the questions "What is the total number of inflection points?" and "Where are they located?" An inability to deal with the inflection points on phase boundaries in a rigorous manner brings another complication. Let us imagine an undulate phase boundary (or its metastable continuation), *i.e.*, the boundary with one or several inflection points. From the thermodynamic viewpoint, a wavy boundary is not illegal; it usually indicates that the excess entropy of at least one of the coexisting phases strongly depends on temperature. Let us now focus on a particular inflection point. Is it physically feasible, or is it an artifact resulting from inappropriate phase models stemming, in turn, from the CALPHAD method? In many cases, the existence of the inflection point is fully justified. If, for instance, the liquid phase has a metastable miscibility gap below liquidus, then a corresponding liquidus line may possess an inflection point, which abscissa is close to (but not necessarily coincides with) the abscissa of the top of the immiscibility cupola. Inflection points may appear even if all phases participating in equilibrium are internally stable. It is shown in [9] that when the ideal liquid solution is in equilibrium with a stoichiometric compound, an undulate liquidus is favored by a small entropy of fusion of the compound. In general, however, the thermodynamic arguments may be insufficient to judge whether the particular inflection point is somewhat real and normal, or it is a post-optimization phantom. Apparently, non-thermodynamic rationales related to the shape of the phase boundary should be invoked.

3. Geometric structure of functions

Experiments to measure the thermodynamic properties of phases and heterogeneous mixtures, or to find the conditions of phase equilibria inevitably result in discrete quantities. Imagine, for instance, that a differential thermal analysis is employed to establish the location of liquidus in a binary system. In general, liquidus is composed of smooth curves corresponding to various primary precipitates. It can be shown that a T (x) curve corresponding to a particular primary solidification region is twice continuously differentiable. By investigating melts of different compositions, one ends up with a table x_i, Δx_i, T_i, ΔT_i, $i = 1,...,n$, which is a discrete representation of the smooth function T (x). Let us recall that any smooth function has its own shape, which is also named topology or geometric structure. More specifically, a twice continuously differentiable function is characterized by regions of increase and decrease, regions of convexity and concavity. The number and sequence of these regions define its shape. Let us consider the function shown in Figure 1a. By looking at the plot, one instantly concludes that it has two extrema and three inflection points. It is important to realize that for reaching that verdict, it was not even necessary to know that the function was actually $x \exp(- x^2/8)$. Now let us choose a certain number of points randomly spread over the (-8,8) interval and calculate exact function's values at these points. By inspecting the discrete representation of the

function, Figure 1b, one is still able to conclude rather confidently that there are 2 extrema and 3 inflection points. This ability to recognize the function's topology hinges on the fact that there are many randomly selected points. As Figure 1c suggests, the lesser their number, the harder to judge on the shape of the function. Another reason which may cause difficulties in identifying the geometric structure is noisy data. It is apparent from Figures 1d-1f that if the Gaussian noise intensifies, then sooner or later nothing valid can be said about the toplogy of the function represented by discrete data points. Fortunately, in many cases, both a number of experimental points related to a thermodynamic property or a phase boundary and the accuracy of the measurements are sufficient to quantify their geometric structures. It can be argued that sometimes it might be difficult to agree upon the geometric structure, that an analysis of visualized data performed by different individuals may result in diverse opinions. Let us realize, however, that exactly the same argument is applicable to any human-dependent estimation. If, for instance, different experts are asked to characterize systematic and random errors of EMF measurements reported in a particular publication, then their estimations will hardly coincide.

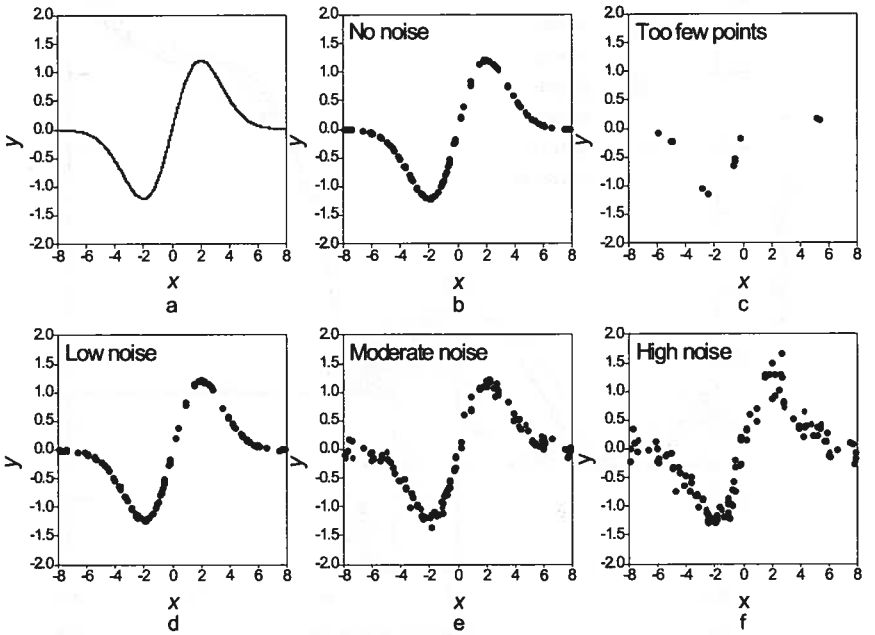

Fig. 1. **a** A twice continuously differentiable function, which geometric structure (2 extrema and 3 inflection points) is obvious **b** A discrete representation of the smooth function still allows a confident determination of its geometric structure **c** A small number of data points makes it difficult or even impossible to rule on the function's topology **d-f** The greater the noise, the more difficult to judge on the geometric structure

If the geometric structure is not apparent from data visualization, then there is no need in invoking a shape-preserving optimization, but if the geometric structure is determinable and determined, then it would be advantageous to take it into account. Mathematically, it means that instead of an unconstrained least-squares problem, one formulates and solves a constrained problem. The objective function is still a sum of weighted residuals between experimental quantities and their calculated counterparts, which means that attention is still paid to the accuracy of description. At the same time, by satisfying topological constraints controlling the shapes of properties and phase boundaries the correctness of a description is assured. In the next section, it is demonstrated how this approach can be implemented in practice.

It would be pertinent to mention that a usefulness of shape-preserving interpolation and approximation was comprehended by mathematicians while ago, and that corresponding algorithms were originated [10-12]. Unfortunately, those elegant methods work only if splines [13, 14] are chosen as functions interpolating or approximating experimental data. Despite an attempt to attract the attention of the CALPHAD community to cubic splines [15], they have not gained popularity in computational thermodynamics so far.

4. Example of a shape-preserving thermodynamic assessment

In 1997, Degterov, Pelton and L'Ecuyer published a thermodynamic assessment of the Se-As system [16]. It was an outstanding work in many respects. Firstly, the authors critically analyzed all available calorimetric and phase diagram data and sagaciously concluded that As_4 Se_4 melted congruently. That conclusion could not be reached by taking into account only the conditions of phase equilibria. Secondly, in addition to the descriptions of the properties of the condensed phases, Degterov *et al.* reported the thermodynamic properties of all gaseous species. Thirdly, their thermodynamic model provided a very good agreement between experimental and calculated quantities. The phase diagram captured from [16] is shown in Figure 2. Two things are worth noticing.

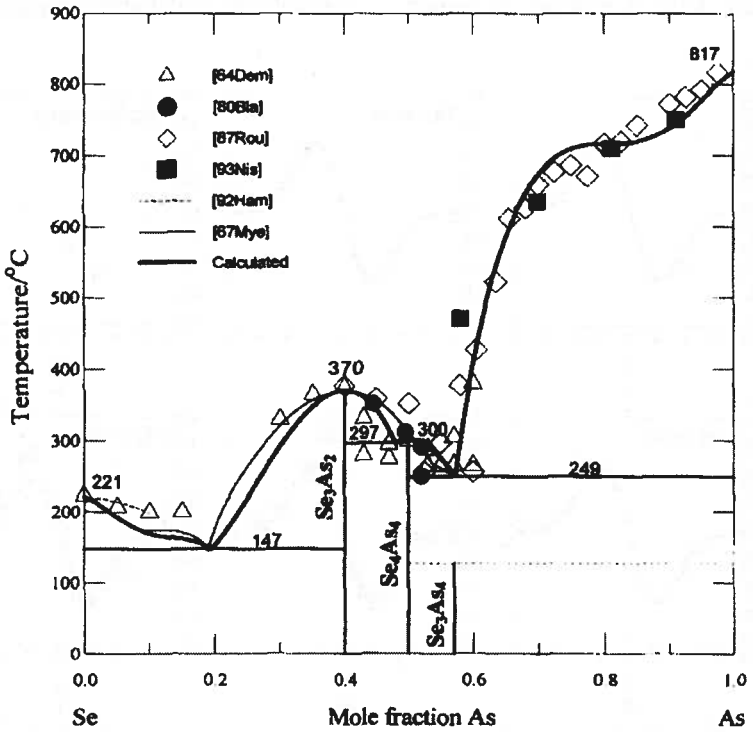

Fig. 2. The phase diagram of the Se-As system resulted from the thermodynamic description of the system proposed in [16]

Firstly, the calculated Se+L/L liquidus is situated far from experimental points obtained in [17] and [18], but this is not a deficiency of the thermodynamic model of the liquid phase. In order to show this, let us recall that since a solid-sate solubility of arsenic in selenium is very small, the slope of the liquidus dT / dx near pure selenium can be calculated as $- RT_m / \Delta_m S$, where $T_m = 494$ K is the melting point of Se and $\Delta_m S = 13.5514$ J /(K × mole) is its entropy of fusion [19]. By using these values, one arrives at $dT / dx \approx -303$K. Since this slope is much steeper than those in [17, 18], it can be guessed that the experimental points are burdened with a systematic error and that, therefore, cannot be trusted. The most likely source of the error is that Se-As melts with $x < 0.6$ are prone to forming glass, which gravely complicates a determination of equilibrium liquidus temperatures within this range.

Secondly, the calculated L/L+As liquidus is undulate: it has two inflection points with $x \approx 0.81$ and $x \approx 0.96$. As Figure 3 illustrates, the left inflection point is linked to a metastable miscibility gap in the liquid phase. This wavy phase boundary does not mean that the thermodynamic description of the liquid phase proposed in [16] is inadequate. A poor accuracy of experimental data and significant differences in the outcomes of the investigations [20] and [21] do not allow one to judge whether the L/L+As liquidus should have one or several inflection points or be completely free of them. Let us notice, however, that if the results of [20] and [21] are analyzed separately, then none of the works suggests that phase boundary is undulate. It is possible that the inflection points appeared, because in [16] data from [20] and [21] were treated simultaneously.

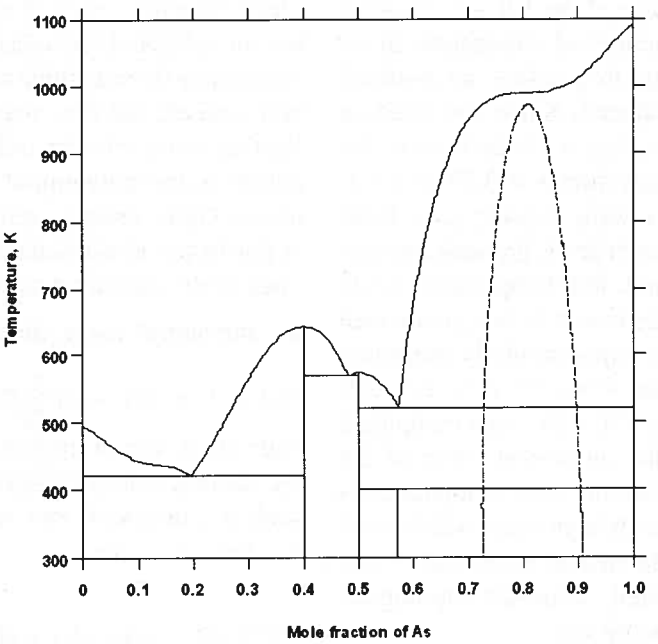

Fig. 3. An undulate L/L+As liquidus is related to a metastable miscibility gap in the liquid phase

Another possible cause of the undulation is that as many as 8 coefficients were used in the expression for the excess Gibbs energy of the liquid phase:

$$G^{ex} = (1-x)\sum_{j=1}^{5} x^j \times L_j = x(1-x)\sum_{j=1}^{5} x^{j-1} \times L_j$$
$$L_1 = -85130.7 + 273.7495T - 34T\ln T \quad L_2 = 59661 \quad L_3 = -680611.9 \quad (1)$$
$$L_4 = 1341023.1 - 10.9083T \quad L_5 = -717983.1$$

It is understood that such a large number of model's parameters was needed in order to achieve a good agreement between the calculated and experimental quantities, but it could happen that the correctness of the description was sacrificed (at least partially) for its accuracy. Instead of continuing these speculations, which, in view of a lack of reliable experimental information on the position of the L/L+As liquidus are senseless and fruitless, let us formulate the following question: Is it in principle possible to optimize the Se-As system in such a manner that this particular liquidus line would be free of inflection point? It should be emphasized that the calculations outlined in this work were attempted not because the quality of the assessment [16] is doubtful. It was undertaken in order to demonstrate that topological constraints introduced in [7, 8] are useful not only for eliminating inverted miscibility gaps, but for suppressing undulations along phase boundaries if such a suppression is warranted by the outcome of the unconstrained minimization technique adopted in the traditional CALPHAD method.

An array of experimental data the re-optimization was based upon coincided with that used by Degterov *et al.* Instead of using raw data on invariant equilibria, it was decided to rely upon values computed in [16]. In other words, it was decided to "nail" a phase diagram that would result from a new method to the following characteristics: eutectic L → Se + Se_3As_2, T = 420.42 K, x = 0.1950; distectic L → Se_3As_2, T = 643.63 K; eutectic L → Se_3As_2 + Se_4As_4, T = 569.69 K, x = 0.4806; distectic L → Se_4As_4, T = 573.54 K; eutectic L → Se_4As_4 + As, T = 521.91 K, x = 0.5736; peritectoid Se_3As_4 → Se_4As_4 + As, T = 399.99 K
The minimization problem was formulated in a habitual CALPHAD fashion:

$$\sum_{i=1}^{m} \omega_i (P_i^{experimental} - P_i^{calculated}(\vec{C}^{Phase_1}, ..., \vec{C}^{Phase_{K_i}})) \rightarrow \min, \quad (2)$$

where m is a number of experimental points, ω_i is the statistical weight of the i - th measurement, P is a property, $\vec{C}$ is the vector of unknown parameters in the expression for the excess Gibbs energy of a corresponding phase, K_i is a number of phases participating in a corre-

sponding equilibrium. The shape of the L/L+As liquidus was directly controlled *via* topological constraints. In order to employ such constraints in practice, an artificial mesh of knots must be introduced. Since the position of the eutectic point L $\rightarrow$ Se_4 As_4 + As is known, the liquidus line of interest stretches from $x \approx 0.57$ to $x = 1$. Within this interval, 42 knots were chosen: $z_1 = 0.58$, $z_2 = 0.59, \ldots, z_{42} = 0.99$. At each knot, liquidus temperature was calculated. In general, that temperature could be compared with nothing, because it is not guaranteed that liquidus temperature was experimentally measured for this composition. Then, the slope dT / dx was calculated. Finally, the curvature d^2T / dx^2 was computed. Of course, there is nothing the numerical value of the curvature can be compared with, but such comparison is not needed! What is needed is its sign only, which must be negative, because it is intended to make the whole liquidus L/L+As convex upward. Thus the topological constraints employed in this work are:

$$(d^2T/dx^2)_{x=z_i} < 0, \quad i = 1, 2, \ldots \quad . \tag{3}$$

It is difficult to give an unambiguous recommendation on a suitable density of the mesh. Apparently, the mesh must be dense enough to avoid an appearance of an inflection point between two adjacent knots. A seemingly excessive number of knots should not be considered as somewhat harmful and slowing the computations down, because usually only a fraction of the topological constraints is active. Moreover, from the algorithmic end, a dense mesh does not significantly increase a computational complexity of the minimization problem. Experience gained suggests that a mesh of equidistant knots with the step $z_{i+1} - z_i \leqslant 0.01$ works almost always.

It should be pointed out that the proposed type of optimization cannot be performed by using the PARROT module [22] of Thermo-Calc, because this software package cannot compute the second derivatives. In order to carry out the topologically-constrained optimization in practice, a Fortran 90 program was written. The heart of this "home-grown optimizer" is the sequential quadratic programming method with augmented Lagrangian line search function developed by Klaus Schittkowski [23].

Before commencing the re-optimization of the Se-As system, it was necessary to decide what particular model or formalism should be used for representing the excess Gibbs energy of the liquid phase. The properties of the components insinuate that a variety of associates may exist in the Se-As melt and that their presence is especially pronounced in a Se-rich liquid phase. From this angle, it would be natural to try the associate solution model [24, 25]. However, one of the purposes of this contribution is to demonstrate that the topological constraints can be used to arrive at the desired shape of a phase boundary even if not a physically feasible model, but an aphysical formalism is in play. The shape-related constraints do not inhale a physical sense into the formalism, indeed, but they may make the outcome of its utilization more reliable and trustworthy. It was decided to adhere to the polynomial spirit of the description of the excess Gibbs energy employed in [16]. That description is not in the Redlich-Kister format, which was incorporated in the optimizer mentioned above. This seems to be an immaterial issue, because $G^{ex} = x(1-x)\sum_{i=0}^{n} \alpha_i(T)x^i$ and $G^{ex} = x(1-x)\sum_{i=0}^{n} \beta_i(T)(1-2x)^i$ are algebraically equivalent, which implies that (1) can be converted into the canonical Redlich-Kister expression. Let us see how such a conversion can be made for the case in hand. According to [16]:

$$G^{ex}/(x(1-x)) = A_{11} + B_{11}T + C_{11}T\ln T + xA_{12} + x^2A_{13} + x^3A_{14} + x^3TB_{14} + x^4A_{15}. \tag{4}$$

Let us absentmindedly replace all x with 1 - 2x and introduce a new set of coefficients $\vec{\alpha}$ and $\vec{\beta}$ instead of the old set $\vec{A}$ and $\vec{B}$ (the term $C_{11}T$ ln T must be left intact, indeed):

$$G^{ex}/(x(1-x) = \alpha_{11} + \beta_{11}T + C_{11}T\ln T + (1-2x)\alpha_{12} + (1-2x)^2\alpha_{13} + (1-2x)^3\alpha_{14} + (1-2)^3T\beta_{14} + (1-2x)^4\alpha_{15}. \tag{5}$$

By comparing the coefficients at corresponding basis functions in (4) and (5), it can be concluded that $-6\beta_{14}xT + 12\beta_{14}x^2T$ must be identical with zero, *i.e.*, that $\beta_{14} \equiv 0$. The absurdity of this requirement evidences that an artless substitution of x with 1 - 2x was not a particularly bright idea. It is clear that in order to translate (4) into the Redlich-Kister format, extra terms are to be added to (5):

$$G^{ex}/(x(1-x) = \alpha_{11} + \beta_{11}T + C_{11}T\ln T + (1-2x)\alpha_{12} + (1-2x)T\beta_{12} + (1-2x)^2\alpha_{13} + (1-2x)^2T\beta_{13} + (1-2)^3\alpha_{14} + (1-2x)^3T\beta_{14} + (1-2x)^4\alpha_{15}. \tag{6}$$

A comparison of the coefficients at corresponding basis functions in (4) and (6) leads to the conclusion that the coefficients in (6) are not linearly independent, because the following two conditions must be satisfied:

$$\beta_{12} + 2\beta_{13} + 3\beta_{14} = 0 \tag{7}$$

$$\beta_{13} + 3\beta_{14} = 0. \tag{8}$$

Although (7) and (8) can be taken into account in the optimizer developed, these two linear dependencies existing between the coefficients were deliberately ignored. By disregarding those interrelationships, a number of adjustable parameters was increased from eight to ten. If it is conjectured that the model for the liquid phase proposed in [16] suffered from overfitting, then two additional terms make the situation even worse. Such state of affairs would be inadmissible, of course, in the case of a non-constrained minimization problem. As will be seen later, by activating the topological constraints, one can overcome an adverse effect of overfitting.

Re-optimization of the Se-As system with the constraints (3) led to the phase diagram depicted in Figure 4. Although the entire L/L+As liquidus is now convex upward, there is an inverted miscibility gap in the liquid phase, which is by far a much more horrible artifact than an undulate liquidus! Fortunately, it has been demonstrated how to use the topological constraints to eliminate inverted miscibility gaps in the course of optimization [7, 8]. That approach was implemented in the present work by introducing a 2D mesh of knots and demanding that the liquid phase must be internally stable at each of these knots. Specifically, four temperatures were chosen: 673.15, 873.15, 1073.15 and 1273.15 K. For each temperature, ninety-nine mole fractions of As were taken: 0.01, 0.02,..., 0.99. At each of 396 knots, it was required that the liquid phase is not prone to separation, *i.e.* that

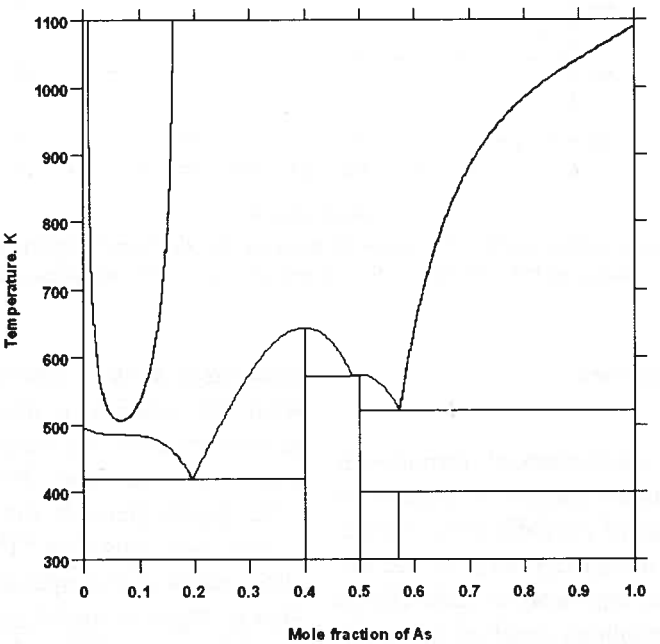

Fig. 4. Although the entire L/L+As liquidus had been made convex upward, a detrimental artifact appeared on the phase diagram

$$\left(\frac{\partial^2}{\partial x^2}(G^{id} + G^{ex})\right)_{T_i,x_j} > 0, \quad i = 1,...,4, j = 1,...,99. \quad (9)$$

It is worth repeating that in spite of a large number of knots, the constraints were likely operative only in a fraction of them.

In Figure 5, the phase diagram resulted from the solution of the minimization problem (2) with two types of topological constraints, (3) and (9), is compared with the diagram from [16]. It is seen that the two phase diagrams are very similar to each other except the position and shape of the L/L+As liquidus. The Gibbs energies of formation of the stoichiometric compounds As_2Se_3, As_4Se_4 and As_4Se_3 are close to those reported by Degterov *et al.* In fact, a new thermodynamic description of the Se-As system is not drastically different from that suggested in [16]. The only principal disparity in the upward convexity of the liquidus line connecting the L → Se_4As_4 + As eutectic point and the point of As melting.

Despite a frequent usage of the term "re-optimization", this work is not aimed at getting a better description of the Se-As system; this work is not indented to discredit the assessment of this system proposed in 1997. The major purpose of this research is to introduce a straightforward method capable of eliminating unwanted or suspicious inflection points at phase boundaries as well as at their metastable continuations during a thermodynamic optimization. A pronouncedly undulate liquidus line in the phase diagram of the Se-As

system made this system a convenient entity to apply the method to. A successful alteration of the excess Gibbs energy of the liquid phase allows one to hope that happy outcomes will be achieved in many other cases when a wavy nature of phase boundaries is less pronounced.

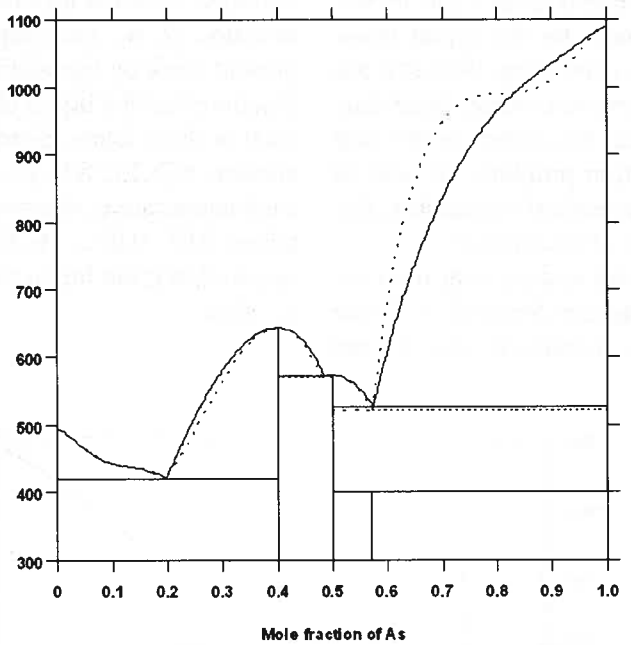

Fig. 5. The phase diagram of the Se-As system (solid lines) resulting from the thermodynamic optimization under topological constraints is very close to that obtained from the traditional CALPHAD method (dashed lines) except the shape and position of the L/L+As liquidus

5. Conclusions

A usage of convenient mathematical formalisms (*e.g.* Redlich-Kister polynomials) instead of physically feasible models (*e.g.* the model of partially ionic liquids [26, 27] or a multi-sublattice model [28, 29]) for the excess Gibbs energies of phases may lead to deficiencies in their thermodynamic descriptions resulted from the CALPHAD method. These deficiencies manifest themselves in various aphysical artifacts [4, 5]. Undoubtedly, the best way to combat them is to employ physically sound models reflecting the properties of the phases. In particular, it is of a paramount importance to take into account the crystallography of solid phases [30-32]. In the case of liquids, a possible formation of associates should not be overlooked. Unfortunately, many phases are so complex (according to [33], a monoclinic unit cell of $Cu_{4.5}Dy$ contains more than 7000 atoms!) or so poorly investigated that the usage of formalisms can hardly be avoided in a foreseeable future.

A pain of getting post-optimization phantoms can be alleviated or even completely subdued by using topological constraints imposed not at experimental data points, but at knots belonging to a specially constructed mesh (or, if necessary, a number of overlapping or non-overlapping meshes). These constraints reflect knowledge about a system of interest, which goes beyond the location of discrete experimental points, *i.e.*, beyond metrics. By means of a "topological enforcement" one can pass, for example, such knowledge as "The liquid phase is not prone to separation within a certain $x-T$ range" or "This solid phase cannot reappear above particular temperature" or "Enthalpy of mixing is always negative and $\Delta_{mix}H(x)$ does not have inflection points" or even "This phase boundary is convex downward if $0.13 < x < 0.37$ and convex downward if $0.44 < x < 0.6$" to a program tailored for the thermodynamic assessment. This approach does not make inventing of new good physical models redundant, indeed, but it provides a much needed balance between the accuracy of a thermodynamic description of a system and its correctness.

Although both here and in [7, 8] a potential of the topological optimization was illustrated on binary cases only, it is conceptually straightforward to generalize the procedure to multicomponent systems.

Despite their apparent usefulness, the shape-related constraints are still considered as somewhat exotic; they are seldom invoked in the course of optimization. The situation will never change unless it becomes possible to use them from within such widely used programs as PARROT [22] and OptiSage [34, 35]. It is naive to ex-

pect that the "home-grown optimizer" developed within the framework of this contribution for illustrative purposes only will ever evolve into a full-fledged software package incorporating numerous models and formalisms and providing convenient visualization, *i.e.*, into the package with the features that PARROT and OptiSage already have.

Appendix

If a binary liquid solution, L, and a binary solid solution, S, are in equilibrium, then the following conditions are fulfilled:

$$\begin{cases} F_1(x^{\mathrm{L}}, x^{\mathrm{S}}, T) \equiv G^{\mathrm{L}} - x^{\mathrm{L}} \frac{\partial G^{\mathrm{L}}}{\partial x^{\mathrm{L}}} - G^{\mathrm{S}} \frac{\partial G^{\mathrm{S}}}{\partial x^{\mathrm{S}}} = 0 \\ F_2(x^{\mathrm{L}}, x^{\mathrm{S}}, T) \equiv G^{\mathrm{L}} + (1 - x^{\mathrm{L}} \frac{\partial G^{\mathrm{L}}}{\partial x^{\mathrm{L}}} - G^{\mathrm{S}} - (1 - x^{\mathrm{S}} \frac{\partial G^{\mathrm{S}}}{\partial x^{\mathrm{S}}} = 0. \end{cases} \quad (10)$$

Since F_1 and F_2 remain equal to zero if the equilibrium is maintained, one can use implicit differentiation to arrive at:

$$\Phi_i(x^{\mathrm{L}}, x^{\mathrm{S}}, T) \equiv \frac{\partial F_i}{\partial x^{\mathrm{L}}} + \frac{\partial F_i}{\partial x^{\mathrm{S}}} \frac{\mathrm{d}x^{S}}{\mathrm{d}x^{\mathrm{L}}} + \frac{\partial F_i}{\partial T} \frac{\mathrm{d}T}{\mathrm{d}x^{\mathrm{L}}} = 0, i = 1, 2. \quad (11)$$

By realizing that (11) is a system of linear equations with respect to $\mathrm{d}x^{\mathrm{S}} / \mathrm{d}x^{\mathrm{L}}$ and $\mathrm{d}T / \mathrm{d}x^{\mathrm{L}}$ and by solving it, one gets $\mathrm{d}T / \mathrm{d}x^{\mathrm{L}}$, *i.e.*, the slope of liquidus.

Since Φ_1 and Φ_2 also remain equal to zero if the phases stay in equilibrium, one can continue using implicit differentiation for arriving at:

$$\frac{\partial \Phi_i}{\partial x^{\mathrm{L}}} + \frac{\partial \Phi_i}{\partial x^{\mathrm{S}}} \frac{\mathrm{d}x^{S}}{\mathrm{d}x^{\mathrm{L}}} + \frac{\partial \Phi_i}{\partial T} \frac{\mathrm{d}T}{\mathrm{d}x^{\mathrm{L}}} = 0, i = 1, 2. \quad (12)$$

By recollecting how are defined in (11), one can rewrite (12) as:

$$\frac{\partial}{\partial x^{\mathrm{L}}} \left(\frac{\partial F_i}{\partial x^{\mathrm{L}}} + \frac{\partial F_i}{\partial x^{\mathrm{S}}} \frac{\mathrm{d}x^{\mathrm{S}}}{\mathrm{d}x^{\mathrm{L}}} + \frac{\partial F_i}{\partial T} \frac{\mathrm{d}T}{\mathrm{d}x^{\mathrm{L}}} \right) + \frac{\partial}{\partial x^{\mathrm{S}}} \left(\frac{\partial F_i}{\partial x^{\mathrm{L}}} + \frac{\partial F_i}{\partial x^{\mathrm{S}}} \frac{\mathrm{d}x^{\mathrm{S}}}{\mathrm{d}x^{\mathrm{L}}} + \frac{\partial F_i}{\partial T} \frac{\mathrm{d}T}{\mathrm{d}x^{\mathrm{L}}} \frac{\mathrm{d}x^{\mathrm{S}}}{\mathrm{d}x^{\mathrm{L}}} \right) + \frac{\partial}{\partial T} \left(\frac{\partial F_i}{\partial x^{\mathrm{L}}} + \frac{\partial F_i}{\partial x^{\mathrm{S}}} \frac{\mathrm{d}x^{\mathrm{S}}}{\mathrm{d}x^{\mathrm{L}}} + \frac{\partial F_i}{\partial T} \frac{\mathrm{d}T}{\mathrm{d}x^{\mathrm{L}}} \right) \frac{\mathrm{d}T}{\mathrm{d}x^{\mathrm{L}}} = 0, i = 1, 2. \quad (13)$$

By taking partial derivatives and keeping in mind that $\partial^2 F_i / \partial x^{\mathrm{L}} \partial x^{\mathrm{S}} \equiv 0$, one can rearrange (13) to a handy form:

$$\frac{\partial F_i}{\partial x^{\mathrm{S}}} \frac{\mathrm{d}^2 x^{\mathrm{S}}}{\mathrm{d}(x^{\mathrm{L}})^2} + \frac{\partial F_i}{\partial T} \frac{\mathrm{d}^2 T}{\mathrm{d}(x^{\mathrm{L}})^2} + \frac{\partial^2 F_i}{\partial (x^{\mathrm{L}})^2} + 2 \frac{\mathrm{d}T}{\mathrm{d}x^{\mathrm{L}}} \frac{\partial^2 F_i}{\partial x^{\mathrm{L}} \partial T} + \left(\frac{\mathrm{d}x^{\mathrm{S}}}{\mathrm{d}x^{\mathrm{L}}} \right)^2 \frac{\partial^2 F_i}{\partial (x^{\mathrm{S}})^2} + 2 \frac{\mathrm{d}x^{\mathrm{S}}}{\mathrm{d}x^{\mathrm{L}}} \frac{\mathrm{d}T}{\mathrm{d}x^{\mathrm{L}}} \frac{\partial^2 F_i}{\partial x^{\mathrm{S}} \partial T} + \left(\frac{\mathrm{d}T}{\mathrm{d}x^{\mathrm{L}}} \right)^2 \frac{\partial^2 F_i}{\partial T^2} = 0, i = 1, 2. \quad (14)$$

Since $\mathrm{d}x^{\mathrm{S}} / \mathrm{d}x^{\mathrm{L}}$ and $\mathrm{d}T / \mathrm{d}x^{\mathrm{L}}$ have been already computed from (11), (14) is a system of linear equations with respect to $\mathrm{d}^2 x^{\mathrm{S}} / \mathrm{d}(x^{\mathrm{L}})^2$ and $\mathrm{d}^2 T / \mathrm{d}(x^{\mathrm{L}})^2$.

There is no need to repeat this tiresome sequence of actions to find the curvature of solidus, it can be calculated from the quantities already known:

$$frac \mathrm{d}^2 T \mathrm{d}(x^{\mathrm{S}})^2 = \left(\frac{\mathrm{d}x^{\mathrm{S}}}{\mathrm{d}x^{\mathrm{L}}} \frac{\mathrm{d}^2 T}{\mathrm{d}(x^{\mathrm{L}})^2} - \frac{\mathrm{d}T}{\mathrm{d}(x^{\mathrm{L}})^2} \right) \Big/ \left(\frac{\mathrm{d}x^{\mathrm{S}}}{\mathrm{d}x^{\mathrm{L}}} \right)^3.$$

A rather generic system of equations (14) becomes specific if particular models G^{L} and G^{S} seen in (10) are made use of.

While calculating slopes and curvatures of phase boundaries, one may encounter a number of interesting complications, but their discussion is beyond the scope of this contribution.

Acknowledgements

The author gratefully acknowledges financial support from the Natural Sciences and Engineering Research Council of Canada (NSERC).

REFERENCES

[1] N. Saunders, A. P. Miodownik, CALPHAD, calculation of phase diagrams: a comprehensive guide, Pergamon, 1998.

[2] H. L. Lukas, S. G. Fries, B. Sundman, Computational thermodynamics: the CALPHAD method, Cambridge University Press, 2007.

[3] H. L. Lukas, E. Th. Henig, B. Zimmermann, CALPHAD **1**, 225-236 (1977).

[4] Y. A. Chang, S. Chen, F. Zhang *et al.*, Progress in Materials Science **49**, 347-366 (2004).

[5] R. Schmid-Fetzer, D. Andersson, P. Y. Chevalier *et al.*, CALPHAD **31**, 38-52 (2007).
[6] G. Kaptay, CALPHAD **28**, 115-124 (2004).
[7] D. V. Malakhov, T. Balakumar, Int. J. Mat. Res. **97**, 517-525 (2006).
[8] D. V. Malakhov, T. Balakumar, Int. J. Mat. Res. **98**, 786-796 (2007).
[9] D. V. Malakhov, T. Balakumar, CALPHAD **32**, 89-93 (2008).
[10] H. Akima, Journal of the ACM **17**, 589-602 (1970).
[11] C. A. Micchelli, P. W. Smith, J. Swetits, J. D. Ward, Constructive Approximation **1**, 93-102 (1985).
[12] L. D. Irvine, S. P. Marin, P. W. Smith, Constructive Approximation **2**, 129-151 (1986).
[13] C. De Boor, A practical guide to splines, Springer-Verlag, 1978.
[14] P. Dierckx, Curve and surface fitting with splines, Clarendon, 1993.
[15] G. F. Voronin, S. A. Degtyarev, CALPHAD **6**, 217-227 (1982).
[16] S. A. Degterov, A. D. Pelton, J. D. L'Ecuyer, J. Phase Equil. **18**, 357-368 (1997).
[17] S. A. Dembovskii, N. P. Luzhnaya, Zhurnal Neorganicheskoi Khimii **9**, 660-664 (1964).
[18] A. Hamou, J. M. Saiter, J. Bayard *et al.*, Calorimetrie et analyse Thermique **23**, 175-182 (1992).
[19] A. T. Dinsdale, CALPHAD **15**, 317-425 (1991).
[20] J. C. Rouland, C. Souleau, R. Cěolin, J. Thermal Analysis **32**, 547-558 (1987).
[21] L. A. Nisel'son, A. A. Gasanov, A. G. Yaroshevskii, Vysokochistye Veschestva **4**, 56-61 (1993).
[22] B. Jansson, Computer operated methods for equilibrium calculations and evaluation of thermochemical model parameters, Ph.D. Thesis, Royal Institute of Technology, Stockholm, 1984.
[23] K. Schittkowski, Math. Operationsforsch. u. Statist., Ser. Optimization **14**, 197-216 (1983).
[24] F. Sommer, Z. Metallkde **73**, 72-76.
[25] F. Sommer, Z. Metallkde **73**, 77-86.
[26] M. Hillert, B. Jansson, B. Sundman, J. Ågren, Metallurg. Trans. A **16A**, 261-266 (1985).
[27] B. Sundman, CALPHAD **15**, 109-119 (1991).
[28] M. Hillert, L. -I. Staffansson, Acta Chemica Scandinavica **24**, 3618-3626 (1970).
[29] B. Sundman, J. Ågren, J. Phys. Chem. Solids **42**, 297-301 (1981).
[30] K. C. Harry Kumar, I. Ansara, P. Wollants, CALPHAD **22**, 323-334 (1998).
[31] J. Nakano, D. V. Malakhov, G. R. Purdy, CALPHAD **29**, 276-288 (2005).
[32] J. -M. Joubert, Progress in Materials Science **53**, 528-583 (2008).
[33] R. Černý, L. Guéné, R. Wessicken, J. Solid State Chem. **174**, 125-131 (2003).
[34] E. Köningsberger, G. Eriksson, CALPHAD **19**, 207-214 (1995).
[35] http://www.crct.polymtl.ca/factsage/fs_optisage.php.

Received: 20 September 2008.